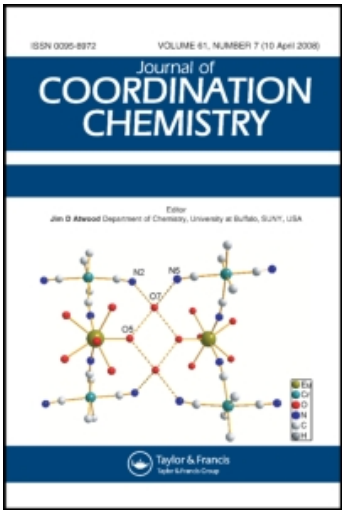


**Journal of Coordination Chemistry**
Publication details, including instructions for authors and subscription information:
http://www.informaworld.com/smpp/title~content=t713455674

# Syntheses, crystal structures of Ni(II), Ag(I)-enoxacin complexes, and their antibacterial activity

Di-Chang Zhong[a]; Zhen-Feng Chen[a]; Yan-Cheng Liu[a]; Xu-Jian Luo[b]; Chrie Barta[c]; Hong Liang[ab]
[a] Key Laboratory for the Chemistry and Molecular Engineering of Medicinal Resources (Ministry of Education of China), School of Chemistry & Chemical Engineering of Guangxi Normal University, Guilin 541004, P.R. China [b] School of Chemistry and Chemical Engineering, Central South University, Changsha 410083, China [c] Division of Pharmaceutics and Biopharmaceutics Faculty of Pharmaceutical Sciences, University of British Columbia, Vancouver, BC, V6 T 1Z3, Canada

First published on: 09 August 2010

**To cite this Article** Zhong, Di-Chang , Chen, Zhen-Feng , Liu, Yan-Cheng , Luo, Xu-Jian , Barta, Chrie and Liang, Hong(2010) 'Syntheses, crystal structures of Ni(II), Ag(I)-enoxacin complexes, and their antibacterial activity', Journal of Coordination Chemistry, 63: 18, 3146 — 3154, First published on: 09 August 2010 (iFirst)
**To link to this Article: DOI:** 10.1080/00958972.2010.507811
**URL:** http://dx.doi.org/10.1080/00958972.2010.507811

*Journal of Coordination Chemistry*
Vol. 63, No. 18, 20 September 2010, 3146–3154



# Syntheses, crystal structures of Ni(II), Ag(I)-enoxacin complexes, and their antibacterial activity

DI-CHANG ZHONG†, ZHEN-FENG CHEN*†, YAN-CHENG LIU†, XU-JIAN LUO‡, CHRIE BARTA§ and HONG LIANG‡†

†Key Laboratory for the Chemistry and Molecular Engineering of Medicinal Resources (Ministry of Education of China), School of Chemistry & Chemical Engineering of Guangxi Normal University, Guilin 541004, P.R. China
‡School of Chemistry and Chemical Engineering, Central South University, Changsha 410083, China
§Division of Pharmaceutics and Biopharmaceutics Faculty of Pharmaceutical Sciences, University of British Columbia, Vancouver, BC, V6 T 1Z3, Canada



(*Received 31 March 2009; in final form 13 May 2010*)

Two metal–enoxacin complexes, $[Ni(H\text{-}Ex)_2(H_2O)_2](NO_3)_2$ (**1**) and $Ag_2(H\text{-}Ex)_4(NO_3)_2$ (**2**) (where H-Ex = enoxacin, Ex = deprotonated enoxacin), have been synthesized and characterized by elemental analysis, infrared spectroscopy, and single crystal X-ray diffraction. Complex **1** is composed of a $[Ni(H\text{–}Ex)_2(H_2O)_2]^{2+}$ core with two uncoordinated nitrates. The Ni(II) lies on the inversion site in a slightly distorted octahedral environment. Complex **2** is a binuclear silver(I) complex, in which two Ag(I) ions are bridged by a weakly bonding bidentate $NO_3^-$. The coordination modes of enoxacin are monodentate for **2** and bidentate for **1**. In addition, **1** and **2** were screened for their activities against several bacteria and showed activities similar to that of free enoxacin; the test compounds were more active against Gram-negative bacteria than Gram-positive bacteria.

*Keywords*: Nickel(II); Silver(I); Crystal structure; Enoxacin; Antibacterial activity

## 1. Introduction

Enoxacin [H-Ex, 1-ethyl-6-fluoro-1,4-dihydro-4-oxo-7-(1-pierazinyl)-1,8-naphtyridine-3-carboxylic acid] (scheme 1), a quinolone derivative, is used in the therapy of infections and shows great activity against Gram-positive and Gram-negative bacteria [1]. The exact mechanism of quinolone action is not yet completely understood; however, it is generally believed that quinolones target the bacterial enzyme gyrase–DNA complex which is responsible for the supercoiling of bacterial DNA [2] (Mitscher's recent review highlights many of these important and sometimes contradictory results [2]). Recent studies also indicate that metal ions may play an important role in the mechanism of action of these drugs [3]. Therefore, the interactions of metal ions with quinolones and

*Corresponding author. Email: chenzfgxnu@yahoo.com

*Journal of Coordination Chemistry*
ISSN 0095-8972 print/ISSN 1029-0389 online © 2010 Taylor & Francis
DOI: 10.1080/00958972.2010.507811

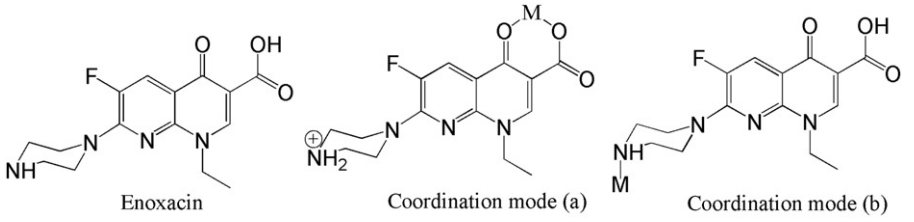


Scheme 1. Molecular structure and coordination modes of enoxacin.

other non-steroidal anti-inflammatory drugs (oxicams) have attracted much attention [4, 5].

According to our previously reported results, quinolones exhibit many different coordination modes, such as chelates through ring carbonyl and carboxylate oxygens to form discrete molecules. In strongly acidic conditions, protonated quinolones appear as cations which readily form ionic metal complexes. In basic media, the quinolones, bearing a piperazine ring in position seven (typical representatives include ciprofloxacin (H-Cif), norfloxacin (H-Norf), pefloxacin, and enoxacin), also form coordination polymers with various dimensions where the terminal piperazinyl nitrogens coordinate to metals [6–12].

Till now, Zn(II) [13], Mg(II) [14], Ca(II) [14], and Tb(III) [15] enoxacin metal complexes have been synthesized and analyzed for their electroanalytical and/or fluorimetric applications. Recently, Arayne and coworkers [16] reported the synthesis, characterization, antibacterial, and anti-inflammatory activities of enoxacin metal complexes. However, only selected transition metal complexes have been crystallographically characterized in the solid state, such as Mn(II) [17], Zn(II) and Co(II) [18–22], and Cu(II) [23, 24]. Herein, we present the synthesis of two metal–enoxacin complexes, their full characterization and antibacterial activity.



## 2. Experimental

### 2.1. *Material and physical measurements*

Analytical grade enoxacin was purchased from *Alfa Aesar* and used as received. All other reagents used were of analytical grade. Microanalyses (C, H, and N) were carried out with a Perkin-Elmer 2400 II elemental analyzer. Infrared (IR) spectra were recorded on a Perkin-Elmer Spectrum One FT-IR Spectrometer. Samples were prepared as KBr discs for the range 4000–400 $cm^{-1}$.

### 2.2. *Synthesis of the complexes*

**2.2.1. $[Ni(H\text{-}Ex)_2(H_2O)_2](NO_3)_2$ (1).** $Ni(NO_3)_2 \cdot 6H_2O$ (1 mmol) and enoxacin (2 mmol) were mixed in solution containing 6 mL ethanol and 12 mL water. After stirring for 30 min, the mixture was placed in a 25 mL Teflon-lined reactor and heated at

110°C in an oven for five days. Blue block crystals were obtained after filtering (*ca* 95% yield). Anal. Calcd for $C_{30}H_{38}F_2N_{10}NiO_{14}$ (%): C, 41.93; H, 4.46; N, 16.30. Found (%): C, 41.92; H, 4.40; N, 16.26. IR (KBr, $cm^{-1}$): 1631(s, $\nu_{as}(COO^-)$), 1608(s, $\nu_{ketone}(C=O)$), 1568(s), 1529(m), 1475(s, $\nu_s(COO^-)$), 1446(s), 1383(s, $\nu(NO_3^-)$).

**2.2.2. $Ag_2$(H-Ex)$_4(NO_3)_2$ (2).** $AgNO_3$ (0.1 mmol) and enoxacin (0.2 mmol) were thoroughly mixed in a mortar with a pestle and placed in a thick-walled Pyrex tube. After addition of 0.1 mL triethylamine and 1 mL anhydrous methanol, the tube was frozen with liquid $N_2$, placed under vacuum, and sealed with a torch. The tube was heated at 60°C for one day to give brown block crystals with a yield of 76% based on enoxacin. Anal. Calcd for $C_{60}H_{68}Ag_2F_4N_{18}O_{18}$ (%): C, 44.46; H, 4.23; N, 15.55. Found (%): C, 44.38; H, 4.20; N, 15.59. Main IR peaks (KBr, $cm^{-1}$): 1629(s, $\nu_{as}(COO^-)$), 1579(m, $\nu_{ketone}(C=O)$), 1474(s, $\nu_s(COO^-)$), 1446(s), 1384(s, $\nu(NO_3^-)$).

### 2.3. *X-ray structure determination*

Crystal data and refinement parameters used in the unit-cell determination and data collection are summarized in table 1 for the two complexes. Intensity data of single crystals were collected on a Bruker SMART CCD area detector diffractometer with graphite-monochromated Mo-K$\alpha$ radiation ($\lambda = 0.71070$ Å) in the $\omega$–$2\theta$ scan mode at 193 K. The structures were solved by direct methods (SHELXS 97) [25] and refined by full-matrix least-squares based on $F^2$ (SHELXL 97) [26]. The non-hydrogen atoms were subject to anisotropic refinement. Hydrogens bound to carbon were calculated theoretically and those bound to oxygen and nitrogen were determined using difference Fourier maps.



### 2.4. *Antibacterial tests*

Antimicrobial activity of enoxacin and the corresponding enoxacin complexes, **1** and **2** (dissolved in 10% DMSO to ensure solubility, the $Ni(NO_3)_2$ and $AgNO_3$ solutions being used as negative controls), were evaluated using the agar diffusion test according to the literature [20, 27]. The minimal inhibitory concentration (MIC) results of these compounds against six bacteria (*Staphylococcus aureus*, *beta-hemolytic streptococcus*, *Streptococcus pneumoniae*, *Escherichia coliform*, *Pseudomona*, *Candida albicans*) are presented in table 2.

## 3. Results and discussion

### 3.1. *Description of the crystal structures*

**3.1.1. [Ni(H-Ex)$_2(H_2O)_2$]·2$NO_3$ (1).** The molecular structure is shown in figure 1 and selected bond distances and angles are tabulated in table 3. Similar to [Ni(H-cip)$_2(H_2O)_2$]$(NO_3)_2 \cdot 2H_2O$ [28], the crystal structure of **1** is mononuclear with Ni(II) in a distorted octahedral coordination environment. The equatorial plane is composed of

Table 1. Crystal data and refinement details for **1** and **2**.

| | $[Ni(H\text{-}Ex)_2(H_2O)_2](NO_3)_2$ (**1**) | $Ag_2(H\text{-}Ex)_4(NO_3)_2$ (**2**) |
|---|---|---|
| Empirical formula | $C_{30}H_{38}F_2N_{10}NiO_{14}$ | $C_{60}H_{68}Ag_2F_4N_{18}O_{18}$ |
| Formula weight | 859.41 | 1621.06 |
| Temperature (K) | 193(2) | 193(2) |
| Crystal system | *Triclinic* | *Triclinic* |
| Space group | $P\bar{1}$ | $P\bar{1}$ |
| Unit cell dimensions (Å, °) | | |
| $a$ | 8.715(3) | 13.9580(16) |
| $b$ | 8.986(2) | 14.0449(12) |
| $c$ | 12.619(3) | 18.3028(13) |
| $\alpha$ | 92.308(3) | 67.778(10) |
| $\beta$ | 109.915(5) | 76.436(12) |
| $\gamma$ | 111.492(5) | 82.500(12) |
| Volume (Å$^3$), $Z$ | 849.0(4), 1 | 3225.4(5), 2 |
| $Z$ | 1 | 2 |
| $D_{Calcd}$ (Mg m$^{-3}$) | 1.681 | 1.669 |
| Absorption coefficient (mm$^{-1}$) | 0.671 | 0.707 |
| Crystal size (mm$^3$) | 0.20 × 0.15 × 0.10 | 0.39 × 0.28 × 0.12 |
| $\theta$ range for data collection (°) | 3.02–25.34 | 3.01–25.35 |
| Data/parameters | 3091/269 | 11726/928 |
| $R$ indices [$I > 2\sigma(I)$] | $R_1 = 0.0397$<br>$wR_2 = 0.0881$ | $R_1 = 0.066$<br>$wR_2 = 0.1326$ |
| $R$ indices (all data) | $R_1 = 0.0500$<br>$wR_2 = 0.0936$ | $R_1 = 0.0923$<br>$wR_2 = 0.1462$ |

Table 2. MIC values (μg mL$^{-1}$) of **1** and **2** for bacteria and fungi assayed.

| Microorganism | Enoxacin | **1** | **2** | $Ni(NO_3)_2$ | $AgNO_3$ |
|---|---|---|---|---|---|
| *S. aureus* | 1.42 | 4.38 | 3.47 | 512.00 | 4.00 |
| *Beta-hemolytic streptococcus* | 5.65 | 68.99 | 13.87 | No data | No data |
| *S. pneumoniae* | 2.83 | 136.98 | 27.74 | 256.00 | 4.00 |
| *E. coliform* | 0.36 | 0.55 | 0.44 | 512.00 | 64.00 |
| *Pseudomona* | 1.42 | 4.38 | 3.47 | 256.00 | 4.00 |
| *C. albicans* | 1445.75 | 136.98 | 221.88 | > 512.00 | 64.00 |

**1** = $[Ni(H\text{-}Ex)_2(H_2O)_2](NO_3)_2$; **2** = $Ag_2(H\text{-}Ex)_4(NO_3)_2$.

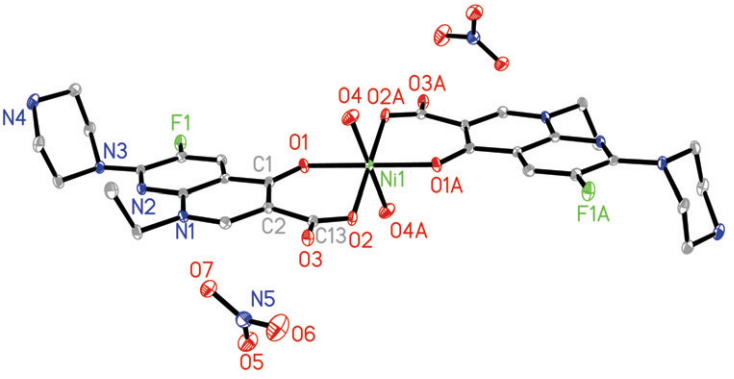


Figure 1. ORTEP drawing of **1**.

Table 3. Selected bond lengths (Å) and angles (°) for **1**.

| | | | |
|---|---|---|---|
| Ni(1)–O(1) | 2.0289(16) | O(1)–Ni(1)–O(1 A) | 180.00(10) |
| Ni(1)–O(2) | 2.0275(17) | O(2)–Ni(1)–O(4) | 87.37(8) |
| Ni(1)–O(4) | 2.059(2) | O(1)–Ni(1)–O(2) | 89.21(6) |
| | | O(1) – Ni(1)–O(2 A) | 90.79(6) |
| O(1)–Ni(1)–O(4) | 89.89(7) | O(1 A)–Ni(1)–O(2) | 90.79(6) |
| O(1)–Ni(1)–O(4 A) | 90.11(7) | O(2)–Ni(1)–O(2 A) | 180.00(8) |

Symmetry transformations used to generate equivalent atoms: A $-x, -y, -z$.

four oxygens, two from the quinolone ring and the other two from carboxylate, forming a stable six-membered chelate ring (coordination mode (a)). Two water molecules occupy the apical positions and the $NO_3^-$ remains uncoordinated. Due to two hydrogens attached to N(2), the protonated nitrogen of piperidyl ring has no coordination capacity, making **1** a typical zwitterion. The Ni(1)–O(1) and Ni(1)–O(2) bond distances are nearly identical (2.0289 and 2.0275 Å, respectively); however, the Ni(1)–O(4) bond distance is slightly longer (2.059 Å). The O(1)–Ni(1)–O(2) and O(1)–Ni(1)–O(4) angles vary from 89.21° to 89.89°, respectively. Bond distances and angles of enoxacin ligand are within the normal range [29]. Hydrogen bonds weave **1** into a supramolecular network (figure 2), where all possible donor hydrogens actively participate including water, the protonated amino group, the uncoordinated carboxylate, and fluorine (table 4).



**3.1.2. $Ag_2(H\text{-}Ex)_4(NO_3)_2$ (2).** As shown in figure 3, $Ag_2(H\text{-}Ex)_4(NO_3)_2$ (**2**) is composed of a $[Ag(H\text{-}Ex)_2]^+$ cation, a neutral $Ag(H\text{-}Ex)_2(NO_3)$ moiety, and two $NO_3^-$ (which weakly bridge the two neighboring silver metal ions in a bidentate fashion). Similar to $Ag(H\text{-}Norf)_2(NO_3)$ [11], the H-Ex ligand in **2** is neutral monodentate (coordination mode (b)) coordinating Ag(1) and Ag(2) by nitrogen of the piperidyl ring. The 4-oxo and 3-carboxylate oxygens of enoxacin remain uncoordinated. The coordination mode of enoxacin in **2** differs from silver perfloxacin, in which two silvers are joined in dimeric pairs by bridging coordinating carboxyl groups from two perfloxacin molecules. The piperazinyl nitrogen from another perfloxacin also coordinates to each silver [12]. The local coordination environment around Ag(1) is angular [N(4)–Ag(1)–N(8) 165.06(16)°]. The deviation from 180° is attributed to weak interaction between Ag(1) and $NO_3^-$. Ag(2) is considered to be four-coordinate by the weakly coordinated $NO_3^-$ and two nitrogens of the neutral H-Ex ligands that occupy two apices of the distorted tetrahedron. The separation of Ag(1) and Ag(2) is 5.4583(7) Å, which implies no metal–metal interaction. Both H-Ex ligands maintain their original geometry, similar to that of the free ligand [29]. Strong intramolecular hydrogen bonds (2.478–2.550 Å) were observed between O(1) and O(2), O(4) and O(5), O(10) and O(11), as well as between O(13) and O(14), thought to have prevented the carboxylate groups from coordinating to Ag. The bond distances of Ag–N, Ag–O and angles of N–Ag–N, N–Ag–O are comparable to those of $Ag(H\text{-}Norf)_2(NO_3)$ [11] and $\{[Ag_4(H\text{-}Cip)_2(Cip)_2(NO_3)_2]\cdot 4H_2O\}_n$ [30] (table 5). Other geometric parameters of enoxacin are in the normal range [29]. Hydrogen bonds produced between the protonated amino groups, the uncoordinated

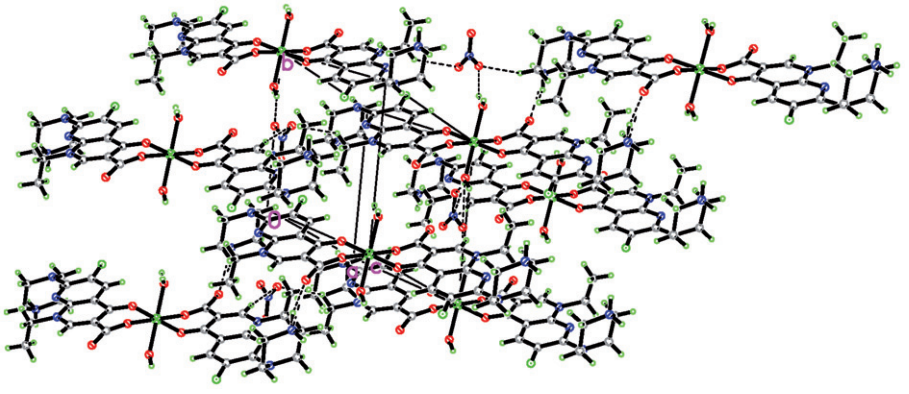

Figure 2. Packing view of **1**.

Table 4. Hydrogen bonds for **1** [(Å) and (°)].

| D–H···A | *d*(D–H) | *d*(H···A) | *d*(D···A) | ∠(DHA) |
|---|---|---|---|---|
| O(4)–H(4D)···O(6)#2 | 0.818(10) | 2.024(14) | 2.812(3) | 162(3) |
| O(4)–H(4C)···N(5)#3 | 0.823(10) | 2.613(17) | 3.360(3) | 152(3) |
| O(4)–H(4C)···O(6)#3 | 0.823(10) | 2.58(3) | 3.153(3) | 128(3) |
| O(4)–H(4C)···O(5)#3 | 0.823(10) | 1.964(13) | 2.772(3) | 167(3) |
| C(14)–H(14B)···O(7)#4 | 0.99 | 2.53 | 3.277(3) | 132.0 |
| C(12)–H(12B)···F(1) | 0.99 | 2.10 | 2.831(3) | 129.6 |
| C(11)–H(11B)···O(2)#5 | 0.99 | 2.49 | 3.110(3) | 120.2 |
| C(11)–H(11A)···O(7)#6 | 0.99 | 2.59 | 3.058(3) | 108.9 |
| C(10)–H(10A)···O(6)#5 | 0.99 | 2.58 | 3.394(4) | 139.7 |
| C(3)–H(3)···O(7) | 0.95 | 2.40 | 3.337(3) | 169.7 |
| N(4)–H(4B)···O(3)#6 | 0.92 | 1.91 | 2.794(3) | 161.9 |
| N(4)–H(4A)···O(3)#5 | 0.92 | 1.85 | 2.704(3) | 154.3 |

Symmetry transformations used to generate equivalent atoms: #2 $-x+1, -y+1, -z$; #3 $x-1, y, z$; #4 $-x+2, -y+1, -z+1$; #5 $x, y, z+1$; #6 $-x+1, -y+1, -z+1$.



carboxylate, and fluorine (table 6) weave **2** into a 2-D supramolecular layer in the *ab*-plane (figure 4).

### 3.2. *Infrared spectra*

Chelation of the metal to enoxacin can be easily observed in IR spectra of the metal complexes when compared to the IR spectrum of the free enoxacin. The broad split band observed between 3600 and 2400 $cm^{-1}$ in spectra of the metal complexes is attributed to the O–H and the N–H stretching vibrations of the piperazinyl moiety [31]. Very strong peaks at 1630, 1600, and approximately 1470 $cm^{-1}$, in addition to the absence of a strong $\nu$(COOH) band above 1700 $cm^{-1}$ corresponding to free enoxacin [20], indicate that the carboxylic acid of enoxacin is deprotonated and coordinated to the metal ions in **1**. The ketone participates in bonding to the Ni(II) shifting to lower wavenumber at 1568 $cm^{-1}$ for **1** [21]. A strong, broad peak at 1343 $cm^{-1}$ for **1** indicates the presence of an uncoordinated $NO_3^-$.

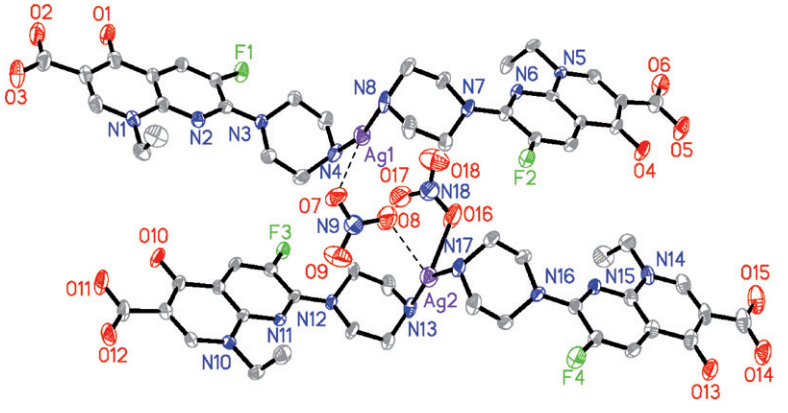


Figure 3. ORTEP drawing of **2**.

Table 5. Selected bond lengths (Å) and angles (°) for **2**.

| | | | |
|---|---|---|---|
| Ag(1)–N(8) | 2.177(4) | N(8)–Ag(1)–N(4) | 165.06(16) |
| Ag(1)–N(4) | 2.186(4) | N(13)–Ag(2)–N(17) | 156.75(16) |
| Ag(2)–N(13) | 2.182(4) | N(13)–Ag(2)–O(16) | 99.34(17) |
| Ag(2)–N(17) | 2.204(4) | N(17)–Ag(2)–O(16) | 97.48(17) |
| Ag(2)–O(16) | 2.588(4) | | |

Table 6. Hydrogen bonds for **2** [(Å) and (°)].

| D–H···A | *d*(D–H) | *d*(H···A) | *d*(D···A) | ∠(DHA) |
|---|---|---|---|---|
| O(4)–H(4D)···O(6)#2 | 0.818(10) | 2.024(14) | 2.812(3) | 162(3) |
| O(4)–H(4C)···N(5)#3 | 0.823(10) | 2.613(17) | 3.360(3) | 152(3) |
| O(4)–H(4C)···O(6)#3 | 0.823(10) | 2.58(3) | 3.153(3) | 128(3) |
| O(4)–H(4C)···O(5)#3 | 0.823(10) | 1.964(13) | 2.772(3) | 167(3) |
| C(14)–H(14B)···O(7)#4 | 0.99 | 2.53 | 3.277(3) | 132.0 |
| C(12)–H(12B)···F(1) | 0.99 | 2.10 | 2.831(3) | 129.6 |
| C(11)–H(11B)···O(2)#5 | 0.99 | 2.49 | 3.110(3) | 120.2 |
| C(11)–H(11A)···O(7)#6 | 0.99 | 2.59 | 3.058(3) | 108.9 |
| C(10)–H(10A)···O(6)#5 | 0.99 | 2.58 | 3.394(4) | 139.7 |
| C(3)–H(3)···O(7) | 0.95 | 2.40 | 3.337(3) | 169.7 |
| N(4)–H(4B)···O(3)#6 | 0.92 | 1.91 | 2.794(3) | 161.9 |
| N(4)–H(4A)···O(3)#5 | 0.92 | 1.85 | 2.704(3) | 154.3 |

Symmetry transformations used to generate equivalent atoms: #2 $x-1, y, z$; #3 $-x, -y, -z+1$; #4 $-x-1, -y, -z+2$; #5 $-x+1, -y, -z+1$; #6 $-x, -y+1, -z+2$.

### 3.3. *Antibacterial activity*

Table 2 shows MICs of **1** and **2** against Gram-positive bacteria, Gram-negative bacteria, and fungi. Compared with free enoxacin, these complexes show slightly lower activity against Gram-positive bacteria and similar activity against Gram-negative bacteria. MIC values of **1** and **2** are higher than the proligand enoxacin and show excellent activity against *C. albicans*. Against *S. aureus*, *S. pneumoniae*, *E. coliform* and

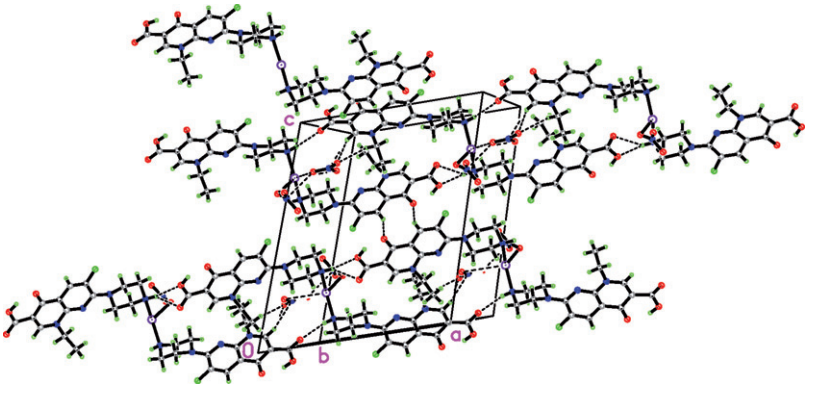


Figure 4. Packing view of **2** viewed in the *ab*-plane.



*Pseudomona* the MIC values of **1** are remarkably lower than that of $Ni(NO_3)_2$. Against *S. pneumoniae* and *C. albicans* the MIC values of **2** are higher than that of $AgNO_3$, but against *E. coliform* the MIC value of **2** is lower than that of $AgNO_3$. For *S. aureus* and *Pseudomona*, **2** and $AgNO_3$ exhibit similar activity. Against *S. aureus* and *E. coliform*, **1** and **2** show lower MIC values than those of $Co(H\text{-}Ex)_2(ClO_4)_2 \cdot 3H_2O$ and $Co(H\text{-}Ex)_2(NO_3)_2 \cdot 2H_2O$ [20]. All these results indicate that for enoxacin coordinated to metal ions, the antibacterial activity is very complicated, in some cases the activity is enhanced, but other cases it is reduced or similar.

## 4. Conclusion

Ni(II) and Ag(I)-enoxacin complexes have been synthesized and characterized by X-ray single crystal diffraction. **1** is a mononuclear, bidentate Ni(II) complex; **2** is a binuclear, monodentate Ag(I) complex. The activity of the two complexes against the various bacterial strains are similar to that of enoxacin, suggesting that the metal may not play a significant role in the antimicrobial efficiency of the metal complexes except for the heightened efficiency of **1** and **2** against *C. albicans*. Although the exact reason for the differences in toxicity between the metal complexes and against different bacterial strains is not known, it is postulated that it is due to the varying coordination surroundings and the differences in the metals tested. In the near future, we hope to further probe the exact reason for these differences.

## Supplementary materials

Crystallographic data for the crystal structures of **1** and **2** reported in this article have been deposited with the Cambridge Crystallographic Data Center (CCDC No. 672149, 672150), respectively. These materials can be obtained free of charge *via* www.ccdc.

cam.ac.uk/conts/retrieving.html (or from the CCDC, 12 Union Road, Cambridge CB2 1EZ, UK; Fax: +44 1223 336033; Email: deposit@ccdc.cam.ac.uk).

## Acknowledgments

The authors thank the National Natural Science Foundation of China (No. 20861002), 973 Plan of China (2009CB526503) and the Natural Science Foundation of Guangxi Province of China (No. 0991012Z, 0991003), and the Open Foundation of the Key Laboratory for the Chemistry and Molecular Engineering of Medicinal Resources (Ministry of Education of China) for financial support.

## References

[1] K. Satto, Y. Inoue, T. Fujii, H. Aoyama, M. Inoue. *Antimicrob. Agents Chemother*., **30**, 777 (1986).
[2] L.A. Mitscher. *Chem. Rev*., **105**, 559 (2005).
[3] J. Robles, J. Martin Polo, L. Álvarez Valtierra, L. Hinojosa, G. Mendoza-Díaz. *Met.- Based Drugs*, **7**, 301 (2000).
[4] I. Turel. *Coord. Chem. Rev*., **232**, 27 (2002).
[5] N.E.A. El-Gamel. *J. Coord. Chem*., **62**, 2239 (2009).
[6] Z.F. Chen, R.G. Xiong, J.-L. Zuo, Z. Guo, X.-Z. You, H.-K. Fun. *J. Chem. Soc., Dalton Trans*., 4013 (2000).
[7] Z.-F. Chen, B. Li, Y.-R. Xie, R.-G. Xiong, X.-Z. You, X.-L. Feng. *Inorg. Chem. Commun*., **4**, 346 (2001).
[8] Z.-F. Chen, R.-G. Xiong, J. Zhang, X.-T. Chen, Z. Xue, X.-Z. You. *Inorg. Chem*., **40**, 4075 (2001).
[9] Z.-F. Chen, L.-C. Yu, D.-C. Zhong, H. Liang, X.-H. Zhu, Z.-Y. Zhou. *Inorg. Chem. Commun*., **9**, 839 (2006).
[10] Z.-F. Chen, H. Liang, H.-M. Hu, Y. Li, R.-G. Xiong, X.-Z. You. *Inorg. Chem. Commun*., **6**, 241 (2003).
[11] R.-X. Li, Z.-F. Chen, R.-G. Xiong, Z. Xue, H.-X. Ju, X.-Z. You. *Inorg. Chem. Commun*., **6**, 819 (2003).
[12] N.-C. Baenziger, C.L. Fox Jr, S.L. Modak .. *Acta Cryst*., **C42**, 1505 (1986).
[13] Z.-R. Qu, H. Zhao, L.-X. Xing, X.-S. Wang, Z.-F. Chen, Z. Yu, R.-G. Xiong, X.-Z. You. *Eur. J. Inorg. Chem*., 2920 (2003).
[14] L.-Z. Wang, Z.-S. An, J.-Q. Wang, X.-L. Zhang, H.-L. Huang. *J. Indian Chem. Soc*., **78**, 305 (2001).
[15] H.R. Park, K.Y. Chung, H.C. Lee, J.K. Lee, K.M. Bark. *Bull. Korean Chem. Soc*., **21**, 849 (2000).
[16] S. Arayne, N. Sultana, U. Haroon, M.A. Mesaik. *Bioinorg. Chem. Appl*. DOI: 10.1155/2009/914105 (2009).
[17] F.-T. You, L.-P. Jin, H.-C. Zhao. *Anal. Commun*., **36**, 231 (1999).
[18] L.-C. Yu, Z.-F. Chen, C.-S. Zhou, H. Liang, Y. Li. *J. Coord. Chem*., **58**, 1681 (2005).
[19] L.-C. Yu, Z.-F. Chen, M.-X. Tan, H. Liang, C.-S. Zhou, Y. Zhang. *Chin. J. Chem*., **24**, 899 (2006).
[20] N. Jiménez-Garrido, L. Perelló, R. Ortiz, G. Alzuet, M. González-Álvarez, E. Cantón, M. Liu-González, S. García-Granda, M. Pérez-Price. *J. Inorg. Biochem*., **99**, 677 (2005).
[21] L.-C. Yu, L. Lai, S.-L. Liu, Y. Xia. *J. Coord. Chem*., **62**, 2616 (2009).
[22] L.-C. Yu, L. Lai, R. Xia, S.-L. Liu. *J. Coord. Chem*., **62**, 1313 (2009).
[23] L.-C. Yu, L. Lai, S.-L. Liu, Y. Xia. *J. Coord. Chem*., **62**, 2261 (2009).
[24] L.-C. Yu, L. Lai, S.-L. Liu, Y. Xia. *J. Coord. Chem*., **62**, 903 (2009).
[25] G.M. Sheldrick. *SHELXTL V5.1, Software Reference Manual*, Bruker AXS, Madison, WI (1997).
[26] G.M. Sheldrick. *SHELXS-97 and SHELXL-97*, University of Göttingen, Germany (1997).
[27] I. Turel, A. Sõnc, M. Zupančič, K. Sepčić, T. Turk. *Met.-based Drugs*, **7**, 101 (2002).
[28] L.-C. Yu, Z.-F. Chen, H. Liang, C.-S. Zhou, H.-K. Fun. *J. Coord. Chem*., **59**, 953 (2006).
[29] Y.-C. Yu, H. Liang, C.-S. Zhou, Z.-F. Chen, Y. Zhang. *Acta Cryst*., **E60**, o1051 (2004).
[30] Z.-F. Chen, L.-C. Yu, D.-C. Zhong, H. Liang, X.-H. Zhu, Z.-Y. Zhou. *Inorg. Chem. Commun*., **9**, 839 (2006).
[31] M.P. López-Gresa, R. Ortiz, L. Perelló, J. Latorre, M. Liu-González, S. García-Granda, M. Pérez-Pried, E. Cantón. *J. Inorg. Biochem*., **92**, 65 (2002).